

Analysis and Design of Double-mitered Right-angle Bend based on Planar Circuit Model and Rigorous Equivalent Network

Yasuhiro AKIMOTO Takaharu HIRAOKA Jui-Pang HSU

Faculty of Engineering, Kanagawa University, Yokohama Japan

Abstract- Strip-line right-angle bend is a key component for MIC. It has been demonstrated that right-angle bend with proper cut can improve the frequency characteristics of no-cut right-angle bend. However their characteristics are deteriorated with frequency, which can be improved again by double-mitered structure. In this paper how to analyze the double-mitered right-angle bend is explained based on 2-D planar circuit model and rigorous equivalent network. The analysis demonstrates the mechanism of no reflection and guideline for design. Also effective equivalent network of 45 degree planar junction for dominant mode will work well for analysis and design of the double-mitered structure. Finally dynamic behavior of 2-D field distribution is calculated and shown, which will help to understand the operation of double-mitered bend.

Keywords- Stripline double-mitered right-angle bend, 45 degree planar junction, eigenvalue, Foster-type equivalent network, equivalent network for dominant mode, phase characteristic

I. INTRODUCTION

Stripline right-angle bend is one of the key components for MIC. Analysis by 2-D planar circuit model^[1] demonstrates that frequency characteristics of right-angle bend with no cut shown in Fig.1(a) can be improved to realize low reflection and wider band-width by square-shaped cut shown in Fig.1(b)^[2] and improved further by slantwise cut as shown in Fig.1(c)^{[3],[4]}. However, their frequency characteristics are deteriorated with frequency and these structure can not realize low reflection at higher frequency. Double-mitered bend as shown in Fig.1(d) can solve this problem; reflection by first 45 degree planar junction can be cancelled by the reflection caused by second junction, resulting in no reflection at all. So far how to design the structure (determination of the length of middle strip-line connecting two mitered bends) is not clear. The reason is that performance of single mitered bend (45 degree) is roughly known^{[5],[6]}, but effect of coupling between two discontinuities is not known. Hence in this paper rigorous equivalent network is introduced based on planar circuit model, and is applied to the calculation of the frequency characteristics and analysis of operation, through which effect of two discontinuities and mechanism of no-reflection at input port are investigated. The results of these analysis will give how to determine the length of strip-line for realizing no reflection at the desired frequency. Also equivalent network for single mitered bend (45 degree) is introduced and shown to be useful for not short strip-line case where higher mode coupling can be neglected. Finally, dynamic 2-D field distribution is calculated and demonstrated. Through the analysis $W=W_0$ in Fig.2(a) is assumed.

II. EQUIVALENT NETWORK BY MODE THEORY

Stripline double-mitered right-angle bend shown in Fig.2(a) can be modelled to planar circuit with magnetic side wall. Then, the structure is divided into three planar waveguides and two 45 degree planar junctions. Equivalent network for planar waveguide is given by multi-transmission line as in Fig.2(b) whose network parameters (mode propagation constant and mode characteristic

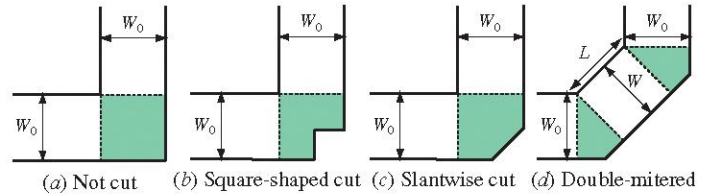


Fig.1 Various stripline right-angle bend

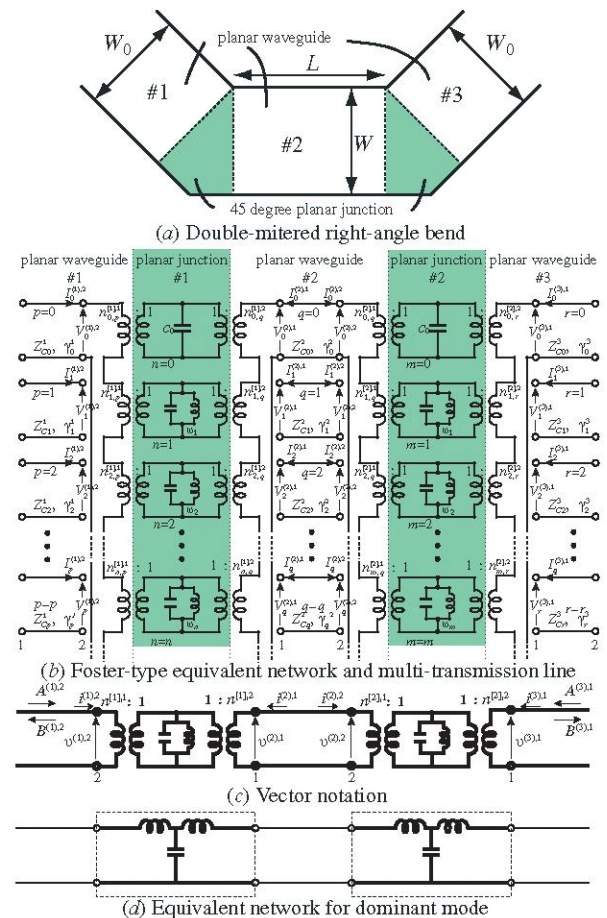


Fig.2 Right-angle bend and its equivalent network

Table 1 Network parameters for equivalent network

Stripline	$c_p^{(i)}(s^i) = \sqrt{\epsilon_p} \cos \frac{p\pi}{W^i} s^i$		$(p = 0, 1, 2, \dots, P)$	(Propagation mode function)
	$\gamma_p^i = \sqrt{(p\pi/W^i)^2 - \omega^2 \epsilon \mu_i}$		$Z_{C_p^i} = \frac{j\omega \mu_i}{\gamma_p^i W^i}$	(Mode characteristic impedance)
Planar junction	$C_0 = \epsilon \frac{S}{d}$ [F] $L_n = \frac{\epsilon \mu}{k_n^2 C_0}$ [H] $\omega_n = \frac{k_n}{\sqrt{\epsilon \mu}}$			(Foster – type equivalent)
	$n_{np}^i = \frac{1}{W^i} \int_0^{W^i} \phi(x, y) c_p^{(i)}(s^i) ds$			
$n^{[j]i} = [n_{np}^i]$				

impedance) are given in Table 1. Foster-type equivalent network for planar junctions is also shown in Fig.2(b), whose equivalent network parameters are derived by solving eigenmode of the corresponding 45 degree planar junction and given by Table 2. Therefore whole equivalent network for stripline double-mitered right-angle bend is given by Fig.2(b) or Fig.2(c) in vector notation. By the way eigenmode of the 45 degree planar junction has been solved by 3-stage configuration and double symmetry with magnetic wall^[4]. Eigenmodes up to 60th are calculated, whose eigenvalues are in Table 2 and field distribution $\phi_n(x,y)$ of lower eigenmodes up to 10th are shown in Fig.3. Also whole equivalent network for dominant mode approximation is shown in Fig.2(d), where equivalent network of single 45 degree planar junction given by T-type networks^[6] is used.

III. CIRCUIT ANALYSIS FOR RIGHT-ANGLE BEND

Double-mitered right-angle bend is analyzed by equivalent network given in Fig.2(c) and circuit theory, where mode voltage/current column vector of j -th port in i -th planar waveguide are defined as $\mathbf{v}^{(i),j}$, $\mathbf{i}^{(i),j}$ in order to consider higher mode of planar waveguide. Then, following matrix relation (1) is given among mode voltage/current column vector of two planar junctions based on mode impedance matrix of 45 degree planar junction, whose element is given by eq.(2).

$$\begin{bmatrix} \mathbf{v}^{(1),2} \\ \mathbf{v}^{(3),1} \\ \mathbf{v}^{(2),1} \\ \mathbf{v}^{(2),2} \end{bmatrix} = \begin{bmatrix} Z^{1,1} & 0 & Z^{1,2} & 0 \\ 0 & Z^{2,2} & 0 & Z^{2,1} \\ Z^{2,1} & 0 & Z^{2,2} & 0 \\ 0 & Z^{1,2} & 0 & Z^{1,1} \end{bmatrix} \begin{bmatrix} \mathbf{i}^{(1),2} \\ \mathbf{i}^{(3),1} \\ \mathbf{i}^{(2),1} \\ \mathbf{i}^{(2),2} \end{bmatrix} \quad (1)$$

$$Z^{i,j} = \left(Z_{p,q}^{i,j} \right) \quad Z_{p,q}^{i,j} = j \frac{1}{C_0} \sum_{n=0}^{\infty} \frac{\omega}{\omega^2 - \omega_n^2} \cdot n_{np}^i \cdot n_{nq}^j \quad (2)$$

where $Z^{1,1} = Z^{2,2}$, $Z^{1,2} = \left(Z^{2,1} \right)^t$

When external mode voltage/current matrix \mathbf{v}^e , \mathbf{i}^e and internal mode voltage/current matrix \mathbf{v}^i , \mathbf{i}^i are introduced by eq.(3), eq.(1) is transformed to eq.(4).

$$\mathbf{v}^e = \begin{bmatrix} \mathbf{v}^{(1),2} \\ \mathbf{v}^{(3),1} \end{bmatrix} \quad \mathbf{i}^e = \begin{bmatrix} \mathbf{i}^{(1),2} \\ \mathbf{i}^{(3),1} \end{bmatrix} \quad \mathbf{v}^i = \begin{bmatrix} \mathbf{v}^{(2),1} \\ \mathbf{v}^{(2),2} \end{bmatrix} \quad \mathbf{i}^i = \begin{bmatrix} \mathbf{i}^{(2),1} \\ \mathbf{i}^{(2),2} \end{bmatrix} \quad (3)$$

$$\begin{bmatrix} \mathbf{v}^e \\ \mathbf{v}^i \end{bmatrix} = \begin{bmatrix} Z^{ee} & Z^{ei} \\ Z^{ie} & Z^{ii} \end{bmatrix} \begin{bmatrix} \mathbf{i}^e \\ \mathbf{i}^i \end{bmatrix} \quad (4)$$

Moreover, the internal mode voltage and current is related by #2 planar waveguide which gives following relation through transmission line theory.

$$\mathbf{v}^i = -Z^i \mathbf{i}^i \quad (5)$$

$$Z^i = \begin{bmatrix} Z_C^{(2)} \coth \gamma^{(2)} L & Z_C^{(2)} \cosh \gamma^{(2)} L \\ Z_C^{(2)} \cosh \gamma^{(2)} L & Z_C^{(2)} \coth \gamma^{(2)} L \end{bmatrix}$$

Therefore, the effective external impedance matrix Z_{eff}^e is given by eq.(6).

$$\mathbf{v}^e = \left[Z^{ee} - Z^{ei} (Z^{ii} + Z^i)^{-1} Z^{ie} \right] \mathbf{i}^e = Z_{eff}^e \mathbf{i}^e \quad (6)$$

When incident and reflected mode voltage matrix at external I/O ports in Fig.2(c) \mathbf{A}^e , \mathbf{B}^e are defined by eq.(7), then external mode voltage/current matrix are given by eq.(8).

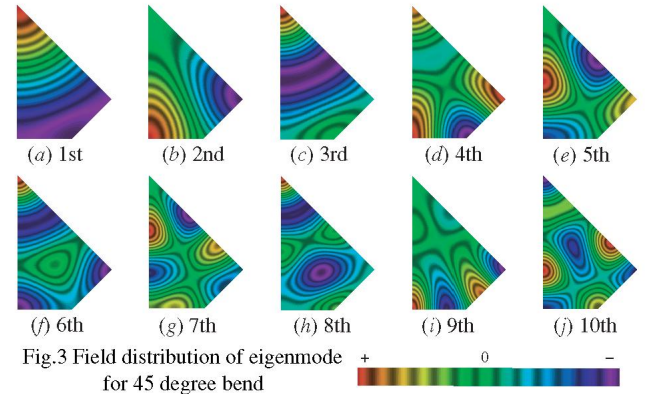
$$\mathbf{A}^e = \begin{bmatrix} \mathbf{A}^{(1),2} \\ \mathbf{A}^{(3),1} \end{bmatrix} \quad \mathbf{B}^e = \begin{bmatrix} \mathbf{B}^{(1),2} \\ \mathbf{B}^{(3),1} \end{bmatrix} \quad Y_C^e = \text{diag}(Y_C^{(1)}, Y_C^{(3)}) \quad (7)$$

$$\mathbf{v}^e = \mathbf{A}^e + \mathbf{B}^e \quad \mathbf{i}^e = Y_C^e (\mathbf{A}^e - \mathbf{B}^e) \quad (8)$$

Substituting eq.(8) into eq.(9) and reorganizing them, voltage scat-

Table 2 Eigenvalue of planar junction ($W=W_0$) $k_n W_0 = \omega_n \sqrt{\epsilon \mu} W_0$

1	3.726576563	16	19.09301094	31	27.29351991	46	34.30639833
2	5.446114404	17	19.0967201	32	28.38061073	47	34.70798204
3	6.789571595	18	20.5010881	33	28.41707264	48	34.7843416
4	9.027583132	19	21.40425922	34	29.12963596	49	35.49455031
5	9.250266053	20	22.07462668	35	29.32690883	50	35.65154293
6	10.0708373	21	22.10930898	36	29.6049937	51	35.9743169
7	12.56658407	22	22.50031776	37	30.61250935	52	36.09227564
8	12.81142971	23	22.52957383	38	31.19492642	53	37.45090533
9	13.64716352	24	23.84474336	39	31.22687865	54	37.50927488
10	13.74382837	25	25.05573413	40	31.61357747	55	37.78382989
11	15.84601346	26	25.1509394	41	31.6145695	56	37.81060305
12	15.89023485	27	25.45142901	42	32.54473153	57	38.28903558
13	16.8798096	28	25.75381158	43	32.6049875	58	38.28924044
14	17.82271497	29	26.59629803	44	33.5000477	59	39.26135858
15	18.24767022	30	26.99355941	45	34.15949315	60	39.29778443



tering matrix which is defined as $\mathbf{B}^e = \mathbf{S}_v \mathbf{A}^e$ is given by eq.(9).

$$\mathbf{S}_v = \left(Z_{eff}^e Y_C^e + \mathbf{I} \right)^{-1} \left(Z_{eff}^e Y_C^e - \mathbf{I} \right) \quad (9)$$

From this equation mode voltage scattering matrix for dominant mode $\mathbf{S}_{v1,1}$ is derived, which leads to give mode voltage scattering matrix for dominant mode as $\mathbf{S}_{p1,1} = \mathbf{S}_{v1,1}$.

IV. FREQUENCY CHARACTERISTICS AND FIELD DISTRIBUTION

Frequency characteristics of the double-mitered right-angle bend are calculated based on rigorous equivalent network of Fig.2(c) and eqs.(6) and (9). Width of the three planar waveguides is $W_0=3.37$ [mm] and relative dielectric constant is $\epsilon_r=2.62$. Calculated frequency characteristics of the power transmission coefficient $S_{p1,1}$ [dB] up to 25[GHz] are shown in Figs.4 and 6(a) with connecting stripline length as a parameter. Through this calculation up to 60th eigenmode of 45 degree planar junction and up to 20th propagation mode of the planar waveguide is taken into consideration. It turns out that double-mitered bend realizes complete transmission at certain discrete frequencies. Also frequency characteristics are calculated based on equivalent network for dominant mode given in Fig.2(d) and shown by dotted line in the same figures for comparison. It turns out that calculated results by dominant mode approximation agree well with exact results for longer stripline but not for 1.0[mm] length. The reason is dominant mode approximation neglects the higher mode coupling and its effect becomes large with shortness of the stripline. 2-D field distribution at operation of no reflection (A) with time phase is calculated and shown in Fig.5.

V. ANALYSIS OF OPERATION

From the calculated results of Fig.4 or Fig.6(a) double-mitered right-angle bend realizes complete transmission at certain discrete frequencies and these discrete frequencies become lower with length of the connecting stripline. This result can be explained by interference cancellation between the reflection of first 45 degree planar junction and that of the second planar junction in double-mitered bend. In order to investigate operating mechanism in detail, practical situation at operation for middle stripline length of $L=5.0[\text{mm}]$ is analyzed in the following.

5-1 The exact frequency characteristics of reflection and transmission for $L=5.0[\text{mm}]$ case shown in Fig.6(a) has two complete transmission at frequency (A) 7.53[GHz] and (C) 21.72[GHz], and relatively low transmission at frequency (B) 16.55 [GHz] whose transmission and reflection coefficient are in Table 3.

5-2 Incident and reflected mode amplitude including higher mode at each port (Fig.6(b)) for unit amplitude incidence of dominant mode at #1 waveguide are calculated and shown in Fig.6(c) with mode order. TEM mode order is "0". It turns out that incident amplitude of higher modes at each port of waveguide #2 is very small because of evanescent attenuation, but reflected amplitude of higher mode is not small because of discontinuity excitation.

5-3 No reflection and complete transmission due to interference cancellation will be proved by practical analysis at (A) and (C) shown in Fig. 6(a). Total reflected amplitude at port 2 of #1 waveguide consists of reflection R_1 by first junction and reflection R_2 by second junction as shown in Fig.7(a). R_1 is estimated by frequency characteristics of single 45 degree planar junction shown in Fig.7(b)^[6]. R_2 (a) is estimated based on Fig.6(b) where multimode coupling is taken into consideration. Estimated results of R_1 and R_2 are plotted in Fig.7(c) for three frequencies (A,B,C), whose numerical value are in Table 4 including sum of R_1 and R_2 . From these results we can see that first reflection is cancelled out by second reflection for case (A), (C) to realize no reflection because their amplitude is the same but their phase 180 degrees difference. Thus complete transmission is proved to be due to the interference cancellation. Also R_2 is estimated by equivalent network for dominant mode approximation given by Fig2(d), whose result is given by eq.(10)

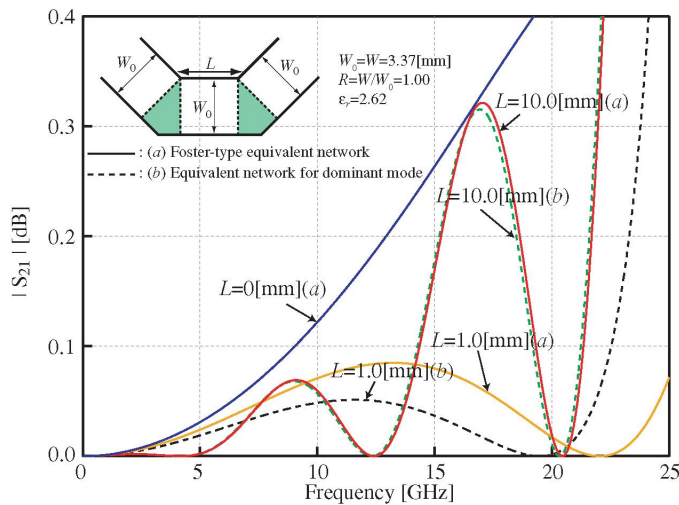


Fig.4 Frequency characteristics for right-angle bend for $L=0, L=1.0, L=10.0[\text{mm}]$

$$R_2 = \frac{1 - (R^2 \exp(-j2\beta L))^N}{1 - R^2 \exp(-j2\beta L)} T^2 \exp(-j2\beta L) \quad (10)$$

where N is number of path through planar waveguide. R_2 of stationary case ($N=\text{infinity}$) for case (A) is calculated and shown in Fig.7(c) by R_2 (b). It is interesting that R_2 (a) of multimode analysis and R_2 (b) of dominant mode analysis is almost the same, which is used the bend design.

5-4 Guideline for design can be given by the previous analysis, which demonstrates that equivalent network for dominant mode is useful. By the way R_2 is again estimated by single path ($N=1$) and infinite path ($N=\text{infinity}$) for case (A) and plotted Fig.7(c), which shows they are almost equal. Hence R_2 is roughly estimated by single path ($N=1$). Then the phase difference of R_1 and R_2 is estimated by the following equation, which can determine the stripline length for the desired center frequency.

$$\text{Phase difference} = 2(\angle T + \beta L) \quad (11)$$

VI. CONCLUSION

It is well-known that double-mitered right-angle bend can realize better transmission compared with other right-angle bend structure. However how to design it is not clear because of two dimensional field problem. Rigorous equivalent network for the double-mitered right-angle bend is formulated by planar circuit model, and applied to the calculation of practical structure and analysis of operation. The analysis demonstrates that the cancellation of reflection by two discontinuities works properly. This analysis show that how to design the double-mitered right-angle bend at the desired center frequency.

Reference

- [1] A.A.Oliner "Equivalent circuits for discontinuities in balanced strip transmission line" pp1134-143 IEEE MTT vol (1954)
- [2] T.Hiraoka, Y. Tabei, K.Kojima, J.P.Hsu "Analysis of stripline right-angle bend with square-shaped corner cut based on eigenmode expansion method and Foster-type equivalent network" APMC'98 WE1B-3
- [3] Hsu, J.P., T.Hiraoka, Y. Tabei " Analysis of stripline right-angle bend with slant-wise corner cut based on eigenmode expansion method and Foster-type equivalent network" IEEE IMS1999 WEF2-2
- [4] T.Hiraoka, Hsu, J.P. "Analysis of Stripline right-angle bend with slantwise corner cut based on Foster-type equivalent network and exact calculation of eigenmode" APMC2001 WE1C-5 pp449-452
- [5] T.Hiraoka, K.Hamatani, J.P.Hsu "Foster-type equivalent network for strip line 45 degrees bend based on calculation of eigenmode and its application" CJMW2004 A-1-10 pp33-36
- [6] T.Hiraoka, K.Hamatani, J.P.Hsu "Calculation of Foster-type equivalent network for stripline 45 degrees bend based on novel calculation method of the eigenmode" EuMC2005

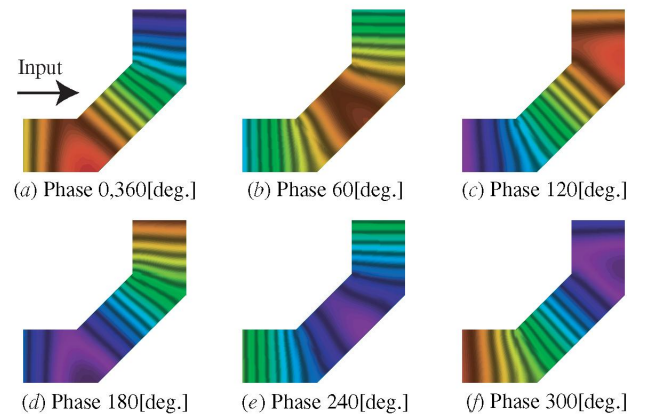
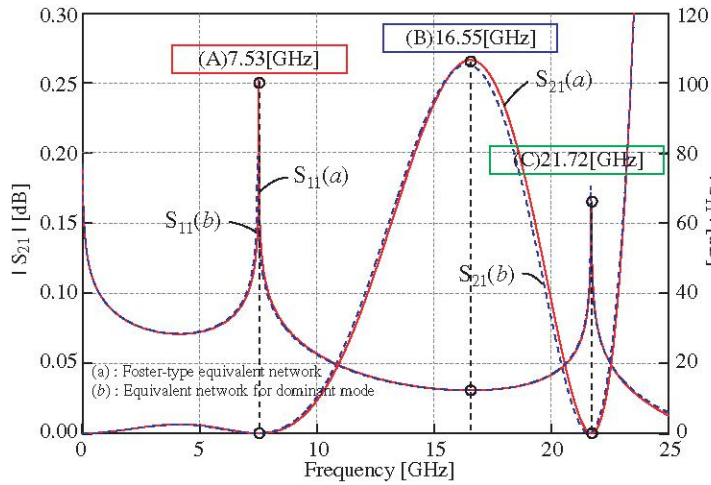
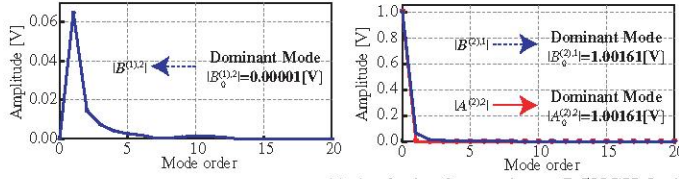


Fig.5 Field distribution at operation of no reflection with time phase ($L=5.0[\text{mm}]$, $F=7.53[\text{GHz}]$)

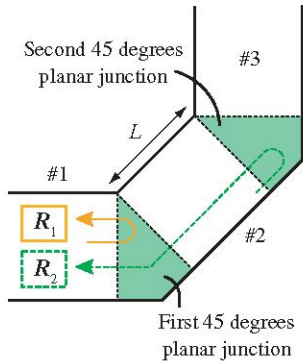


(a) Frequency characteristics for right-angle bend and the middle waveguide length $L=5.0[\text{mm}]$

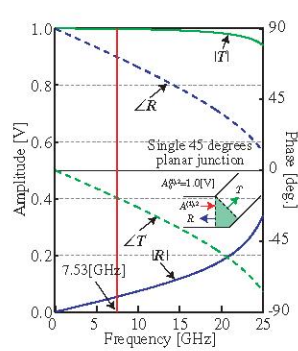


(c) Analysis of operation at 7.53[GHz] --incident voltage and reflected voltage amplitude

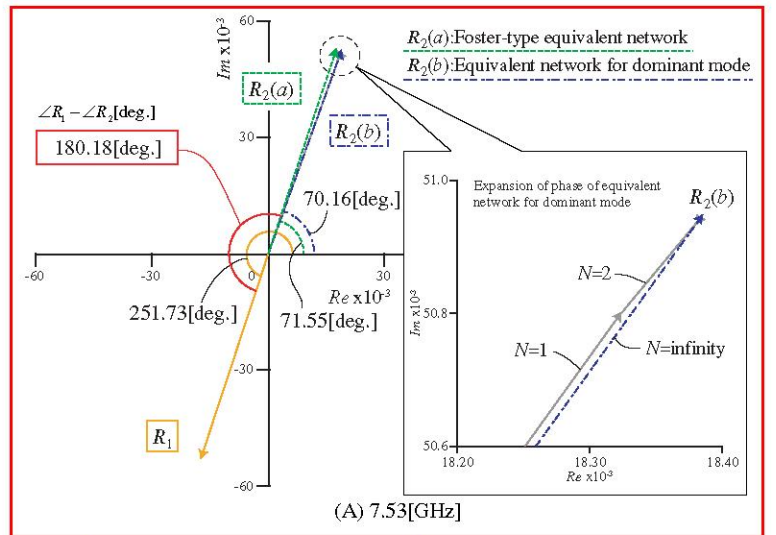
Fig.6 Characteristics of incident/reflected amplitude at each port vs mode order for unit incidence of dominant mode



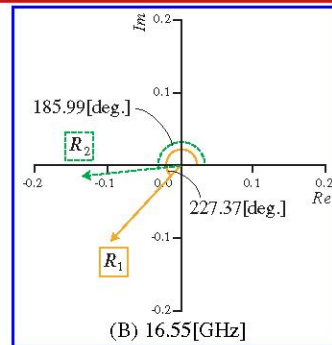
(a) Reflected component of $B^{(1,2)}$



(b) Transmission and reflection of single 45 degrees planar junction



(A) 7.53[GHz]



(c) Phase R_1, R_2 (Dominant Mode)

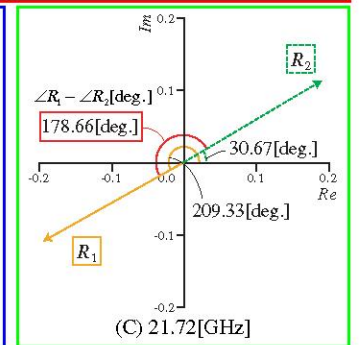


Fig.7 First reflection R_1 and second reflection R_2 at frequency (A),(B) and (C) for operational analysis of complete transmission at (A) and (C)

Table 4 First reflection R_1 , second reflection R_2 and total reflection(=vector sum of both) in amplitude and phase angle representation at frequency (A),(B) and (C)

	(A)	(B)	(C)
F [GHz]	7.53	16.55	21.72
$ R_1 $ [V]	5.42E-02	0.1336	0.2139
$\angle R_1$ [deg.]	251.73	227.37	209.33
$ R_2 $ [V]	5.42E-02	0.1283	0.2141
$\angle R_2$ [deg.]	71.55	185.99	30.67
$\ R_1 - R_2\ $	1.00E-05	0.0053	0.0002
$\angle R_1 - \angle R_2$ [deg.]	180.18	41.38	178.66